



Non-dimensionalized distances and limits for the transition of deflagration to detonation

V. Rodriguez¹ · V. Monnier¹ · P. Vidal¹ · R. Zitoun¹

Received: 9 October 2021 / Revised: 27 April 2022 / Accepted: 25 May 2022 / Published online: 12 July 2022
© The Author(s), under exclusive licence to Springer-Verlag GmbH Germany, part of Springer Nature 2022

Abstract

This experimental work investigates the possibility to non-dimensionalize the limits and the distances of the deflagration-to-detonation transition process (DDT). The deflagration was ignited using jets of hot gases generated by the impact of a Chapman–Jouguet detonation on a multi-perforated plate. The tube was 1 m long with a square cross section $40 \times 40 \text{ mm}^2$. The reactive mixtures were the stoichiometric compositions of hydrogen, methane, and oxygen $(1-x)\text{H}_2 + x\text{CH}_4 + 1/2(1+3x)\text{O}_2$ with the composition parameter x ranging from 0 to 1. The initial pressure p_0 was varied from 12 to 35 kPa, and the initial temperature was 294 K. The widths of the detonation cells and the conditions and distances for DDT were obtained as functions of x , p_0 , the thickness of the plate, and the number and diameter of its perforations. The cell width was used as the reference length. The non-dimensional DDT distances correlate well with the non-dimensional number representing the surface re-ignition effect in the form of a concave increasing function. The non-dimensional DDT limits appear to be independent of the surface dissipation phenomena in the perforations. These trends are found to be independent of the regularity of the detonation cells. DDT processes are very dependent on the system configuration and the ignition conditions, but our analysis suggests that the proper selection of non-dimensional numbers based on the system characteristics can predict the DDT limits and distances to a reasonable approximation.

Keywords Deflagration · Detonation · Cellular structure · Non-dimensionalization · Hot-gas jets

1 Introduction

Understanding the onset of fast flames and their transition to detonation in tubes is one of the oldest motivations for studying quasi-sonic and supersonic combustion waves. The main phenomena that participate in the deflagration and detonation processes, and the transitions from the former to the latter, are well understood qualitatively today. However, the quantitative predictions of their individual or combined behaviors remain a numerical challenge that requires computational capabilities currently out of technological reach. One of the prevailing approaches is to bring out salient relevant parameters for DDT processes based on simplified macroscopic analyses.

Ciccarelli and Dorofeev [1] presented a review of DDT processes that includes the pioneering works by Shchelkin. The DDT phenomenological stages are now agreed to depend on the roughness of the tube walls and the transverse dimension of the tube relative to some reference reaction thickness. Most laboratory DDT processes are triggered using low-energy ignition techniques, such as an automotive spark plug. In smooth tubes with large enough transverse dimensions, the dynamics of the initial flame is then subjected to strong effects of curvature and acceleration, a shock forms ahead of the flame front, an overdriven detonation suddenly forms between the flame and the shock, propagates in the transverse and backward direction with respect to the frontward-propagating leading shock, and this complex eventually relaxes to the CJ detonation regime [2,3]. The overdriven detonation usually forms at the tube wall, preferentially at the inner edges of square or rectangular tubes. This indicates that the dissipation effects in boundary layers also have a strong influence on the flame acceleration; such effects are more effective at wall intersections than at surfaces. For narrow enough tubes and low enough energy of igni-

Communicated by G. Ciccarelli.

✉ V. Rodriguez
vincent.rodriguez@ensma.fr

¹ Institut Pprime, UPR 3346 CNRS, ENSMA, BP 40109, 86961 Futuroscope-Chasseneuil, France

tion, the transition process can include a quasi-steady, slowly accelerating, and quasi-planar combustion wave with velocity about one-half that of the CJ detonation—the so-called strange wave—before sudden one-dimensional transition to the CJ detonation regime, without precursor shock [4–7].

The DDT phenomenon is thus a set of individually complex processes, so there is no single scenario for DDT, and not all phenomena involved in one are relevant to another. A non-exhaustive list of parameters and configurations that participate in DDTs includes the ignition method and power [8], the system geometry (i.e., 1D linear such as in a tube or 1D divergent such as resulting from the point-source ignition of a reactive cloud, etc.). In particular, for the linear geometry, the length and the transverse dimension of the tube and the roughness and the material of its walls (i.e., plastic or metallic) may significantly affect the DDT scenario and characteristic distances. Defects or roughness of the walls may also trigger re-initiation faster than with smooth walls, and obstacles positioned on the flame path are an efficient way to shorten considerably the transition (e.g., the Shchelkin spiral). DDT analyses, including this one, can only be valid for a limited number of scenarios. The objective of our work is thus to conduct and analyze experiments to determine to what extent the proper choice of non-dimensional parameters could represent the transition limits and lengths. Our investigation is restricted to the DDT process generated by jets of hot gases uniformly distributed over most of the cross section of a smooth-wall square tube. These hot jets were obtained from the impact of a CJ detonation on a perforated plate. This choice of surface ignition of the initial subsonic flame front ensures a simpler hydrodynamic field ahead of the front and, therefore, a better reproducibility of the transition limits and lengths. In these conditions, our aim is to obtain macroscopic information on the transition limits and lengths rather than the detailed dynamics of the re-ignition processes.

For similar conditions, the literature review brings out that the main control parameters are the number of holes in the plate, the width λ_{CJ} of the detonation cell, as compared to both the transverse dimension of the tube and the diameter of the holes, and the regularity $\Delta\lambda_{CJ}/\lambda_{CJ}$ of the detonation cells (the standard deviation of their average width). A regularity criterion is defined from the ZND model of the planar detonation reaction zone by the parameter χ defined as the ratio of the reaction thickness to that of the induction zone length [9,10]. This regularity thus increases with decreasing χ . For example, $\chi = 350$ for the mixture $\text{CH}_4 + 2\text{O}_2$ that results in an irregular cell structure and $\chi = 7$ for the mixture $2\text{H}_2 + \text{O}_2$ that results in a regular cell structure at the initial pressure 20 kPa. Overall, the re-ignition distance R decreases with decreasing λ_{CJ} and regularity, that is, re-ignition seems easier with more irregular mixtures [11–14]. The two main re-ignition mechanisms after the incident detonation has quenched through the plate are the interactions

of the diffracted shocks with themselves and the walls of the tube [15–18]. In particular, Medvedev et al. [19] identified (i) a direct detonation initiation in the zone of turbulent mixing between the jets of the combustion products and the fresh mixture and (ii) a detonation initiation from localized explosions resulting from the interaction between the jets and the shock waves reflected off the walls.

Kuznetsov et al. [3] observed that R decreases with decreasing λ_{CJ} for the stoichiometric $\text{H}_2\text{--O}_2$ mixture, and they noted the prominent effect of a turbulent boundary layer before re-ignition. Chao et al. [11] observed that R is shorter for irregular mixtures ($\text{H}_2\text{--Air}$) than with regular mixtures ($\text{H}_2\text{--O}_2$). Sentanuhady et al. [20] used 5-mm-thick perforated plates and diameters d ranging from 1 to 5 mm. They found that R is shorter with multi-perforated plates than with single-hole plates, but they did not detail the effects of the plate thickness and the hole diameter. It should be noted that their plates had hole diameters larger than the cell widths. Grondin and Lee [21] proposed two onset mechanisms based on schlieren visualizations. For regular cells, the reaction zone regenerates within a thin planar layer normal to the main propagation direction without precursor shock. For irregular cells, the regeneration is three-dimensional with distributed burnt and unburnt pockets that coalesce to achieve the CJ detonation regime. Their experimental conditions were such that re-ignition was very close to the plate—about two to three λ_{CJ} , so their results are more representative of the last stage of the DDT process.

The open area ratio (OAR, ratio of the total area of holes to the tube cross-section area) is often considered for characterizing DDT. However, detonation has been often observed to quench inside the perforated plates if the cell width λ_{CJ} is larger or equal to the diameter d of the holes [22–24]. Therefore, the same OAR may, or may not, result in detonation quenching, so the OAR cannot be the only parameter for characterizing DDT ignition.

We determined the transition distances R and limits behind a multi-perforated plate for stoichiometric compositions of hydrogen, methane, and oxygen $(1-x)\text{H}_2 + x\text{CH}_4 + 1/2(1+3x)\text{O}_2$. We varied the composition parameter x from 0 to 1 to generate detonation cells ranging from regular ($x = 0$, $\text{H}_2 + 1/2\text{O}_2$) to irregular ($x = 1$, $\text{CH}_4 + 2\text{O}_2$), according to the usual definition, e.g., [25]. We varied the initial pressure p_0 from 12 to 35 kPa, and the initial temperature was ~ 294 K. We choose perforated plates with hole diameters d smaller than the cell widths λ_{CJ} , so the detonation quenched inside the plate. Therefore, re-ignition behind the plates is from jets of burnt gases. In a first series of experiments, we kept constant the properties of the perforated plates, namely their thickness e , hole number N , and diameter d , and we studied the effects of varying p_0 and the composition parameter x . In a second series of experiments, we selected the more regular mixture, that is, $x = 0$

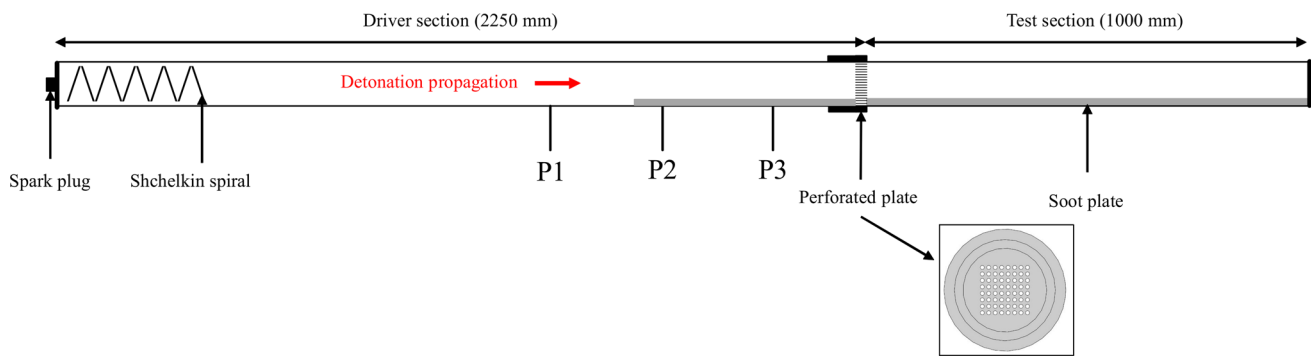


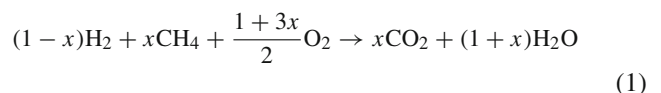
Fig. 1 Schematic of the experimental setup. Channel cross section: $40 \times 40 \text{ mm}^2$, P1, P2, and P3: pressure gauges



Fig. 2 Perforated plate (plate B, Table 1)

2 Experimental methodology

The experimental setup (Fig. 1) is a detonation tube that consists of two main elements, namely the driver section and the re-ignition section, which are separated by a perforated plate (Fig. 2). The methodology is to generate a detonation at one end of the driver section, to quench it through the plate, and to study the conditions for re-ignition depending on the properties of the plate, the composition of the mixture and the initial pressure p_0 . The driver and re-ignition sections are 2.25 and 1 m long, respectively, with square cross section $40 \times 40 \text{ mm}^2$. Figure 1 shows a schematic of the experimental setup, and Table 1 gives the properties of the perforated plates. The detonation in the driver section resulted from the deflagration generated by the spark of an automotive plug, and transition to detonation was promoted by a 1-m-long Shchelkin spiral positioned immediately ahead of the plug. The setup was vacuumed before injecting the premixed composition prepared in a separate tank using the partial pressure method. Three Kistler 603B pressure transducers ($1\text{-}\mu\text{s}$ response time, 300-kHz natural frequency, each coupled with a Kistler 5018 A electrostatic charge amplifier with 200-kHz bandwidth) were used to check that the CJ detonation regime was achieved before the plate. The transducer P3 is located 125 mm before the plate, and the distance between each transducer (P1, P2, and P3) is 250 mm. The reactive mixtures were the stoichiometric compositions of hydrogen–methane–oxygen initially at $T_0 \sim 294 \text{ K}$:



($\text{H}_2 + 1/2\text{O}_2$), and we studied the effects of varying the properties of the perforated plate e , N , and d . We kept constant the open area ratio (OAR) for both series.

Section 2 describes the experimental setup, Sect. 3 presents the analysis of the results that brings out a non-dimensional correlation for the DDT limits and distances based on the properties of the cellular structure and the perforated plate, and the discussion and conclusions of this work are given in Sect. 4.

Table 1 Properties of the perforated plates for generating the hot-gas jets

Plates	Thickness e (mm)	Hole number N	Hole diameter d (mm)	OAR (%)
A	7	64	3	28
B	7	144	2	28
C	14	64	3	28
D	21	64	3	28

Table 2 Composition of the stoichiometric hydrogen–methane–oxygen mixtures $(1-x)\text{H}_2 + x\text{CH}_4 + 1/2(1+3x)\text{O}_2$

No.	x	Composition for $\Phi = 1$	%H ₂	%CH ₄	%O ₂
1	0	H ₂ + 0.5O ₂	0.667	0	0.333
2	0.25	0.75H ₂ + 0.25CH ₄ + 0.875O ₂	0.4	0.13	0.47
3	0.5	0.5H ₂ + 0.5CH ₄ + 1.25O ₂	0.22	0.22	0.56
4	0.75	0.25H ₂ + 0.75CH ₄ + 1.625O ₂	0.095	0.286	0.619
5	1	CH ₄ + 2O ₂	0	0.333	0.667



Fig. 3 Upstream soot-foil recordings showing the detonation cellular structure depending on the composition x of the mixtures $(1-x)\text{H}_2 + x\text{CH}_4 + 1/2(1+3x)\text{O}_2$ at initial pressure $p_0 = 25$ kPa

Five compositions were studied, i.e., $x = 0, 0.25, 0.5, 0.75,$ and 1 (Table 2). Soot-covered foils positioned on the bottom faces of the driver and the re-ignition sections were used to record the structure of the detonation cells upstream and downstream of the plate.

Figure 3 shows soot-foil recordings positioned upstream of the plate, obtained at the initial pressure $p_0 = 25$ kPa. Depending on the composition, that is, the parameter x , the

wall recordings show how the cell width and irregularity increase with increasing x , i.e., with decreasing amount of H₂ and increasing amount of CH₄.

Figure 4 shows a typical soot recording at the position of the final stage of the DDT. Here, the detonation re-ignition occurs at the bottom wall. The cells are first very small, which indicates that this initial detonation is overdriven. They eventually become parallel to the tube axis, with larger and

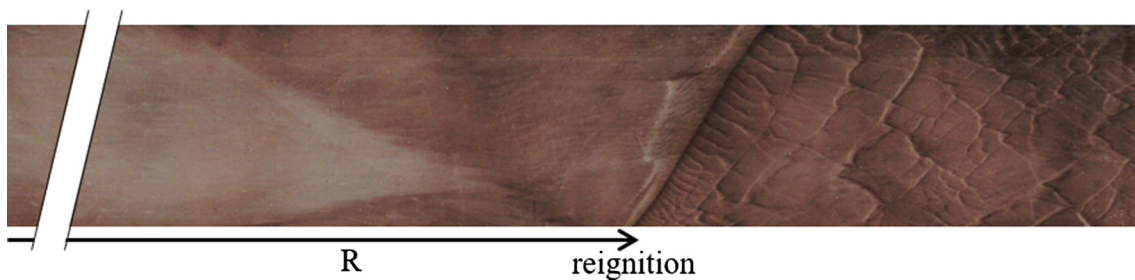


Fig. 4 Downstream soot-foil recording showing detonation re-ignition for the mixture $\text{CH}_4 + 2\text{O}_2$ ($x = 1$) at initial pressure $p_0 = 17.5$ kPa. R is the DDT distance from the perforated plate

essentially constant width, which indicates that the detonation is self-sustained. We also indicate that DDT occurred for all investigated couples (x, p_0) before the frontward-facing shock reaches the end-wall of the tube. The soot recordings indeed indicate unambiguously and easily the wave directions from the grey levels, the detonation cell orientations, and the evolution of their widths. The tube was opened and cleaned after each shot to remove as much soot deposits as possible. Therefore, no re-initiation was due to shock reflection at the closed fixed end of the tube, or due to wall roughness.

3 Results

The premise of the analysis below is that the re-ignition process results essentially from the interplay of two competing phenomena, namely nonadiabatic surface dissipation versus hot spots and chemical heat release, that is, dissipation effects at the tube walls and inner edges versus chemically-enhanced shock amplification. They are described by means of a dimensional analysis that involves chemical and geometrical lengths, namely the cell average width λ_{CJ} , the thickness e , and the diameter d of the holes in the plate. The number of holes N is also an important parameter. Table 1 shows the values of e , d , and N . Surface dissipation takes place at the wall of the holes in the plate and at those of the re-ignition section of the tube, between the plate and the position of re-ignition. The total exchange surface in the plates is $N\pi d e$, and the product $N d e$ is a measure of these nonadiabatic exchanges. This dimensional analysis includes only the contribution of the exchange surface of the holes because it is much larger than that of the tube, per unit length. Further, all experiments were carried out in the same tube, so the results cannot be used to anticipate the re-ignition distances in a tube with a different cross section, wall material, or wall roughness. Hot-gas jets form when the flow exits the holes, and they interact at a distance that depends on the mixture composition and the initial pressure and temperature. The initial total surface of the jets is $N\pi d^2/4$, and the product Nd^2 is a

measure of the surface formed by the interaction of the jets. The analysis considers non-dimensional ratios that use the cell average width λ_{CJ} as the reference length for representing the effect of heat production by evolution of chemical composition. These ratios are (i) $Nd^2/\lambda_{\text{CJ}}^2$ for the relative effects of surface re-ignition resulting from the interaction of the jets coming out of the holes, and (ii) $Ned/\lambda_{\text{CJ}}^2$ for the relative effects of the surface-dissipation phenomenon.

The data were obtained by varying the initial pressure p_0 for a constant composition parameter x . Each couple (x, p_0) was investigated 4 to 7 times, and two sets of measurements were carried out. The data points in the figures below are averages from all couples (x, p_0) regardless of the set. The selected size for the data points is a good indication of the error. Figure 5 shows the cell average width as a function of the composition parameter x . The relationship between cell size and x for a given p_0 turns out to be linear, shown as dashed lines. The p_0 value for each data point is indicated at the right of the dashed line of which the data points are the closest. Some couples (x, p_0) actually show two data points. They are examples of cell average widths obtained for each measurement set. These averages are thus observed close to each other, which is an indication of the good reproducibility of our measurements. The other graphs use averages over the two measurement sets. The cell average width λ_{CJ} thus appears to be a linear increasing function of x at fixed p_0 , and, as is usual, e.g., [26], to increase with decreasing p_0 at fixed x . The curved full line is a convex increasing function of x that interpolates between the closest couples (x, p_0) with DDT (full symbols) and without DDT (open symbols). The limiting pressures at its intersects with the constant- p_0 lines decrease with increasing x , that is, with increasing λ_{CJ} . Therefore, the less regular the cells (the larger x), the smaller the limiting pressure.

Figure 6 shows the domains of re-ignition and non-re-ignition in the plane $Nd^2/\lambda_{\text{CJ}}^2 - Ned/\lambda_{\text{CJ}}^2$. The data were obtained by varying N , d , e , and p_0 , and for the same composition parameter $x = 0$. Each point in the graph corresponds to the change of a single parameter (Table 1). The results suggest that the value of $Nd^2/\lambda_{\text{CJ}}^2$ that separates re-ignition and

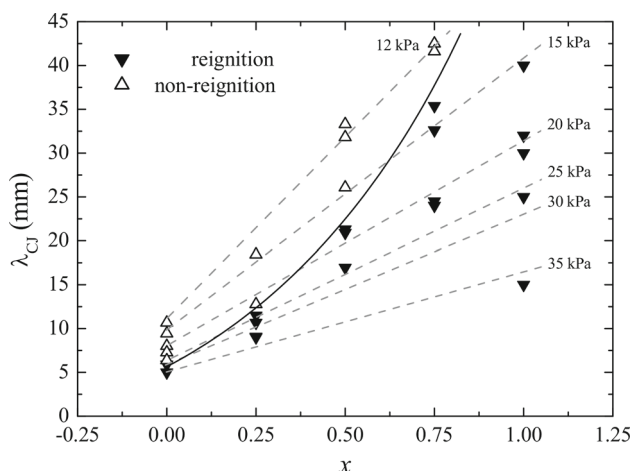


Fig. 5 Re-ignition domain for the mixtures $(1-x)\text{H}_2 + x\text{CH}_4 + 1/2(1+3x)\text{O}_2$ in the plane composition (x)—CJ cell average width (λ_{CJ}) depending on the initial pressure (Plate A, $e = 7$ mm, $N = 64$, $d = 3$ mm, Table 1)

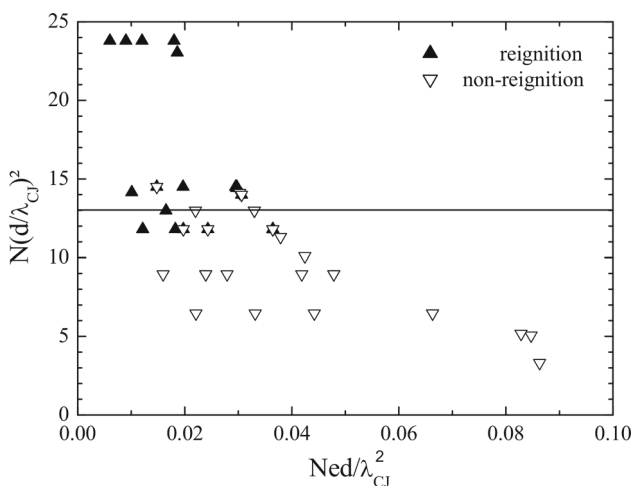


Fig. 6 Non-dimensional re-ignition domain for the mixture $\text{H}_2 + 1/2\text{O}_2$ ($x = 0$) in the plane surface dissipation—re-ignition surface taking into account the properties of all plates (Table 1)

non-re-ignition is independent of the non-dimensional number $Ned/\lambda_{\text{CJ}}^2$. Therefore, within a reasonable accuracy, the limiting non-dimensional number (full line) for the surface re-ignition effects appears to be independent of the non-dimensional number for the surface dissipation effects in the plate. However, as discussed below, the re-ignition distance depends on both effects of the surface dissipation and the surface re-ignition.

For a given composition x of the mixture, the properties of the plate, precisely its nonadiabatic inner processes and the interaction effects at its exit, strongly influence the mechanisms of combustion re-ignition (hot-gas jets, flame structure, and development) and, therefore, the detonation transition distance from the plate. In contrast, the variations

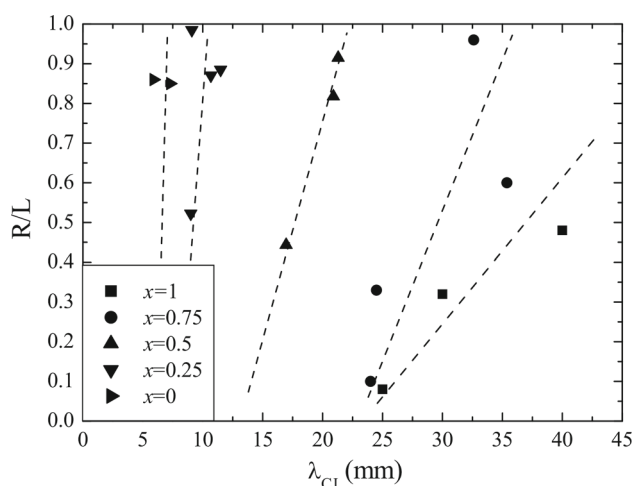


Fig. 7 Non-dimensional re-ignition distance R/L as a function of the average detonation cell size λ_{CJ} for the mixtures $(1-x)\text{H}_2 + x\text{CH}_4 + 1/2(1+3x)\text{O}_2$ (Plate A, $e = 7$ mm, $N = 64$, $d = 3$ mm, Table 1). L is the length of the test section downstream of the perforated plate

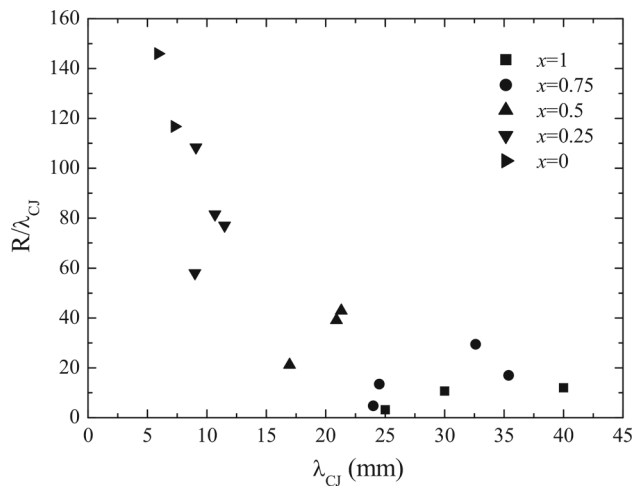


Fig. 8 Non-dimensional re-ignition distance for the mixtures $(1-x)\text{H}_2 + x\text{CH}_4 + 1/2(1+3x)\text{O}_2$ as a function of the cell average width λ_{CJ} (Plate A, $e = 7$ mm, $N = 64$, $d = 3$ mm, Table 1)

of the mixture composition, for the same plate, result in a limited dispersion of the DDT limits and length.

Figure 7 shows the re-ignition distance R as a function of the average width of the detonation cell λ_{CJ} , with the composition parameter x varying from 0 to 1.

The test section length L was the same in all experiments and was used to non-dimensionalize the DDT distance R . From the physical standpoint, longer tubes give longer DDT distances because the rate of initial pressure increase and the formation of the precursor shock obey feedback mechanisms between the piston effect of the flame and the acoustic reflection at the tube end. The rate of initial pressure increase is thus minimum for infinitely long tubes. Of course, DDT cannot be obtained in too short a tube since a shock may form

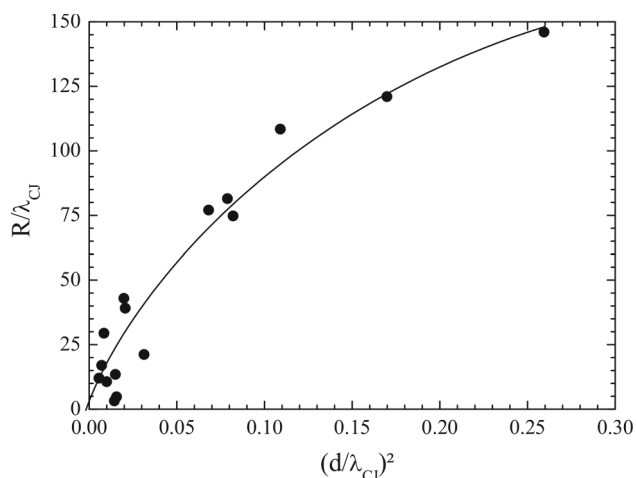


Fig. 9 Non-dimensional re-ignition distance as a function of the re-ignition surface non-dimensional parameter for the mixtures $(1 - x)\text{H}_2 + x\text{CH}_4 + 1/2(1 + 3x)\text{O}_2$ with the values of $x = 0, 0.25, 0.5, 0.75,$ and 1 (Plate A, $e = 7$ mm, $N = 64, d = 3$ mm, Table 1)

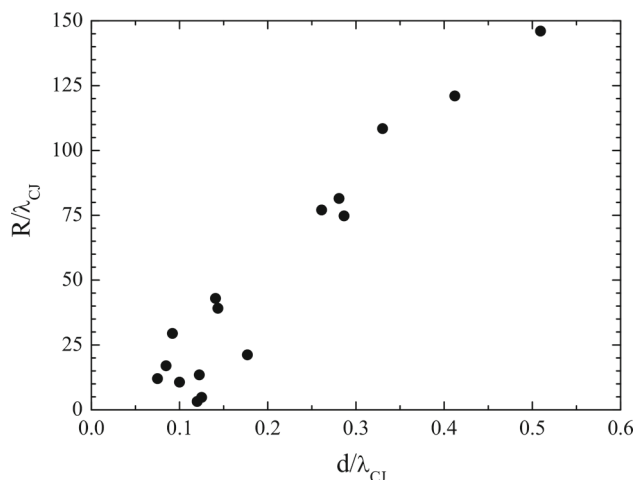


Fig. 10 Non-dimensional re-ignition distance as a function of d/λ non-dimensional parameter for the mixtures $(1 - x)\text{H}_2 + x\text{CH}_4 + 1/2(1 + 3x)\text{O}_2$ with the values of $x = 0, 0.25, 0.5, 0.75,$ and 1 (Plate A, $e = 7$ mm, $N = 64, d = 3$ mm, Table 1)

and reflect at the tube end, thereby generating a backward-propagating shock that interacts with the flame before DDT. In all our experiments, the initiation of the detonation was due to the frontward-propagating shock, which we checked from the analyses of the soot recordings in the test section: the detonation cells unambiguously indicate the propagation direction of the detonation. Many of our DDTs took place in the last 15% of the tube, two in the last 5%, and no reflected shock interacted with the frontward-facing flame. The slopes of the linear fit for each x increase with decreasing x , that is, the transition distance is more sensitive to the cell width for more regular mixtures. Figure 8 also illustrates this trend as the re-ignition distance R non-dimensionalized by λ_{CJ} and plotted as a function of λ_{CJ} .

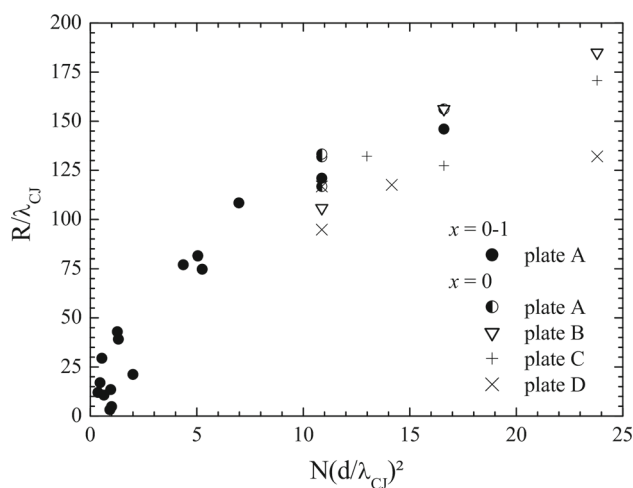


Fig. 11 Non-dimensional re-ignition distance as a function of the re-ignition surface non-dimensional parameter for the mixtures $(1 - x)\text{H}_2 + x\text{CH}_4 + 1/2(1 + 3x)\text{O}_2$ for all plates (Table 1)

Figure 9 shows the non-dimensionalized re-ignition distance R/λ_{CJ} as a function of the non-dimensionalized ratio d^2/λ_{CJ}^2 representing the relative effects of surface re-ignition, for plate (A). A good alignment is observed regardless the value of x (Fig. 10). Figure 11 shows that this property extends to all the plates considered in this study. In our conditions, the thickness of the perforated plate does not appear to significantly influence the re-ignition distance R . Medvedev et al. [19] suggested that this occurs for plate thicknesses e ranging in $e/d = 2 - 8$ (d , the diameter of a hole), and indeed $e/d = 2.33 - 7$ in our experiments. However, we observe that the data spread for the case of plate D with $x = 0$ is slightly larger than for the other cases. We interpret this as the consequence of the large thickness $e = 21$ mm in comparison with the 14- and 7-mm-thick plates. This large value is close to the upper limit of Medvedev’s criterion [19] for independence on the thickness. Figures 10 and 12 show the non-dimensional re-ignition distance R/λ_{CJ} as functions of the square roots of the non-dimensional ratios from Figs. 9 and 11, respectively. They show linear dependencies with the same small spread as Figs. 9 and 11, respectively, which provides indirect proof of the correctness of our physical interpretation with the proposed non-dimensional relative number for surface dissipation.

4 Discussion and conclusions

This paper reports on experiments on the DDT in a square cross-section channel. Our goal was to investigate the possibility of non-dimensionalizing the DDT limits and distances using simple observable characteristic parameters. Ignition was achieved using jets of hot gases generated by quenching

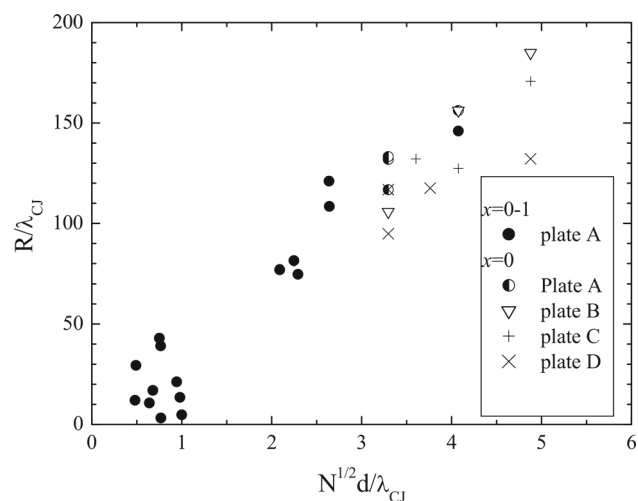


Fig. 12 Non-dimensional re-ignition distance as a function of the $\sqrt{Nd}\lambda_{CJ}$ non-dimensional parameter for the mixtures $(1-x)\text{H}_2 + x\text{CH}_4 + 1/2(1+3x)\text{O}_2$ for all plates (Table 1)

CJ detonation through a perforated plate. Thus, the parameters of our analysis are the CJ cell width, the thickness of the plate, the number and diameter of the holes in the plate, and the composition parameter. For our conditions, the analysis of the data shows that the non-dimensional DDT limits are independent of the relative effects of the surface dissipation phenomenon in the holes, and that the non-dimensional DDT distance correlates well with the non-dimensional number Nd^2/λ_{CJ}^2 representing the relative effects of surface re-ignition resulting from the interaction of the jets coming out of the holes. Additionally, this non-dimensionalization appears to be independent of the cell structure regularity. The regularity criterion may thus not always be relevant for interpreting dynamical behaviors of deflagration and detonation [27,28].

In general, DDT dynamics depends on the ignition mode, the setup geometry and dimensions, and the mixture composition, so only high-resolution numerical simulations based on Navier–Stokes reactive equations will be capable of predicting this complex phenomenon when the necessary computation power becomes available. To date, given an industrial system, the DDT risk must be assessed with large-scale model experiments. In this respect, our analysis suggests that the proper selection of non-dimensional numbers built from the system characteristics can help in anticipating the corresponding DDT limits and distances.

Acknowledgements This work was supported by a CPER-FEDER Project of *Région Nouvelle Aquitaine* and the French National Agency (ANR) under the project ANR-21-CE05-0002-01.

Availability of data and materials The data that support the findings of this study are available from the corresponding author upon reasonable request.

References

- Ciccarelli, G., Dorofeev, S.: Flame acceleration and transition to detonation in ducts. *Prog. Energy Combust. Sci.* **34**, 499–550 (2008). <https://doi.org/10.1016/j.pecs.2007.11.002>
- Kuznetsov, M.S., Matsukov, I., Alekseev, V.I., Breitung, W., Dorofeev S.: Effect of boundary layer on flame acceleration and DDT. CDROM. 20th International Colloquium on the Dynamics of Explosions and Reactive Systems, Montreal (2005)
- Kuznetsov, M.S., Alekseev, V.I., Matsukov, I.: DDT in a smooth tube filled with a hydrogen-oxygen mixture. *Shock Waves* **14**, 205–215 (2005). <https://doi.org/10.1007/s00193-005-0265-6>
- Yanez, J., Kuznetsov, M.S.: Experimental study and theoretical analysis of a ‘strange wave’. *Combust. Flame.* **167**, 494–496 (2016). <https://doi.org/10.1016/j.combustflame.2016.02.004>
- Ssu, H.W., Wu, M.H.: Fomation and characterisation of composite reaction-shock clusters in narrow channels. *Proc. Combust. Inst.* **38**, 3473–3480 (2021). <https://doi.org/10.1016/j.proci.2020.07.069>
- Balossier, Y., Virot, F., Melguizo-Gavilanes, J.: Strange wave formation and detonation onset in narrow channels. *J. Loss Prev. Process Ind.* **72**, 104535 (2021). <https://doi.org/10.1016/j.jlp.2021.104535>
- Balossier, Y., Virot, F., Melguizo-Gavilanes, J.: Flame propagation and acceleration in narrow channels: sensitivity to facility specific parameters. *Shock Waves* **31**, 307–321 (2021). <https://doi.org/10.1007/s00193-021-01015-9>
- Ali Cherif, M., Shcherbanev, S., Starikovskaia, S., Vidal, P.: Effect of non-equilibrium plasma on decreasing the detonation cell size. *Combust. Flame.* **217**, 1–3 (2021). <https://doi.org/10.1016/j.combustflame.2020.03.014>
- Short, M., Sharpe, G.J.: Pulsating instability of detonation with a two-step chain-branching reaction model: theory and numerics. *Combust. Theory Model.* **7**, 401–416 (2013). <https://doi.org/10.1088/1364-7830/7/2/311>
- Radulescu, M.I., Sharpe, G.J., Bradley, D.: A universal parameter quantifying hazards, detonability and hot spot formation: the χ number. *Proceedings of the Seventh International Seminar on Fire and Explosion Hazards*, Singapore (2013)
- Chao, J.: Critical deflagration waves that lead to the onset of detonation. PhD Thesis, McGill University, Montreal, DC, Canada (2006)
- Radulescu, M.I., Sharpe, G.J., Lee, J.H.J., Kiyanda, C.B., Higgins, A.J., Hanson, R.K.: The ignition mechanism in irregular structure gaseous detonations. *Proc. Combust. Inst.* **30**, 1859–1867 (2005)
- Kuznetsov, M.S., Alekseev, V.I., Dorofeev, S.B.: Comparison of critical conditions for DDT in regular and irregular cellular detonation systems. *Shock Waves* **10**, 217–223 (2000). <https://doi.org/10.1007/s001930050009>
- Maley, L., Bhattacharjee, R., Lau-Chapdelaine, S.M., Radulescu, M.I.: Influence of hydrodynamic instabilities on the propagation mechanism of fast flames. *Proc. Combust. Inst.* **35**, 2117–2126 (2015)
- Obara, T., Sentanuhady, J., Tsukada, Y., Ohayagi, S.: Reignition process of detonation wave behind a slit-plate. *Shock Waves* **18**, 63–83 (2008). <https://doi.org/10.1007/s00193-008-0147-9>
- Bhattacharjee, R.R., Lau-Chapdelaine, S.S.M., Maines, G., Maley, L., Radulescu, M.I.: Detonation re-initiation mechanism following the Mach reflection of a quenched detonation. *Proc. Combust. Inst.* **34**, 1893–1901 (2013)
- Ciccarelli, G., Boccio, J.L.: Detonation wave propagation through a single orifice plate in a circular tube. *Twenty-Seventh Symposium (International) on Combustion*, 2233–2239 (1998)
- Zhang, Z., Wang, C., Luo, X., Guo, Y., Rui, S., Guo, W.: Effect of perforated plate with high blockage rate on detonation re-initiation

- in H₂–O₂–Ar mixture. *Int. J. Hydrog. Energy*. **46**(42), 2208–2222 (2021). <https://doi.org/10.1016/j.ijhydene.2021.04.025>
19. Medvedev, S.P., Khomik, S.V., Olivier, H., Polenov, A.N., Bartenev, A.M., Gelfand, B.E.: Hydrogen detonation and fast deflagration triggered by turbulent jet of combustion products. *Shock Waves* **14**, 193–203 (2005). <https://doi.org/10.1007/s00193-005-0264-7>
 20. Sentanuhady, J., Tsukada, Y., Yoshihashi, T., Obara, T., Ohyagi, S.: Re-initiation of detonation waves behind a perforated plate. 20th International Colloquium on the Dynamics of Explosion and Reactive Systems, vol. 20, Montreal, pp. 1–4 (2005)
 21. Grondin, J.S., Lee, J.H.S.: Experimental observation of the onset of detonation downstream of a perforated plate. *Shock Waves* **20**, 381–386 (2010). <https://doi.org/10.1007/s00193-010-0267-x>
 22. Khomik, S.V., Veysiere, B., Medvedev, S.P., Montassier, V., Olivier, V.: Limits and mechanism of detonation re-initiation behind a multi-orifice plate. *Shock Waves* **22**, 199–205 (2012). <https://doi.org/10.1007/s00193-012-0358-y>
 23. Khomik, S.V., Veysiere, B., Medvedev, S.P., Montassier, V., Agafonov, G.L., Silnikov, M.V.: On some conditions for detonation initiation downstream of a perforated plate. *Shock Waves* **23**, 207–211 (2013). <https://doi.org/10.1007/s00193-012-0409-4>
 24. Khomik, S.V., Medvedev, S.P., Veysiere, B., Olivier, H., Maksimova, O.G., Silkikov, M.V.: Initiation and suppression of explosive processes in hydrogen-containing mixtures by means of permeable barriers. *Russ. Chem. Bull.* **63**, 1666–1676 (2014). <https://doi.org/10.1007/s11172-014-0652-1>
 25. Manzhalei, V.I., Mitrofanov, V.V., Subbotin, V.A.: Measurement of inhomogeneities of a detonation front in gas mixtures at elevated pressures. *Combust. Explos. Shock Waves* **10**, 89–95 (1974). <https://doi.org/10.1007/BF01463793>
 26. Strehlow, R.: Investigation of the structure of detonation waves in gases. *Astronautica Acta*. **15**, 345–357 (1970)
 27. Monnier, V., Rodriguez, V., Vidal, P., Zitoun, R.: Experimental analysis of cellular detonations: regularity and 3D patterns depending on the geometry of the confinement. Extended Abstract Accepted for Oral Presentation to the 28th International Colloquium on the Dynamics of Explosion and Reactive Systems, Napoli (2022)
 28. Monnier, V., Rodriguez, V., Vidal, P., Zitoun, R.: An analysis of three-dimensional patterns of experimental detonation cells. Submitted to *Combustion and Flame* (2022)

Publisher's Note Springer Nature remains neutral with regard to jurisdictional claims in published maps and institutional affiliations.